Stokes Drift in Internal Equatorial Kelvin Waves: Continuous Stratification versus Two-Layer Models

JAN ERIK H. WEBER

Department of Geosciences, University of Oslo, Oslo, Norway

KAI H. CHRISTENSEN

Norwegian Meteorological Institute, Oslo, Norway

GÖRAN BROSTRÖM

Department of Earth Science, University of Gothenburg, Gothenburg, Sweden

(Manuscript received 18 June 2013, in final form 16 October 2013)

ABSTRACT

The Stokes drift in long internal equatorial Kelvin waves is investigated theoretically for an inviscid fluid of constant depth. While the Stokes drift in irrotational waves is positive everywhere in the fluid, that is, directed along the phase velocity, this is not always the case for internal Kelvin waves, which possess vorticity. For constant Brunt–Väisälä frequency, the Stokes drift in such waves is sinusoidal in the vertical with a negative value in the middle of the layer for the first baroclinic mode. For a pycnocline that is typical of the equatorial Pacific, this study finds for the first mode that the largest negative Stokes drift velocity occurs near the depth where the Brunt–Väisälä frequency has its maximum. Here, estimated drift values are found to be on the same order of magnitude as those observed in the Pacific Equatorial Undercurrent at the same level. In contrast, a two-layer model with constant density in each layer yields a positive Stokes drift in both layers. This contradicts the fact that, as shown in this paper, the vertically integrated Stokes drift (the Stokes flux) must be zero for arbitrary Brunt–Väisälä frequency.

1. Introduction

The mass transport induced by periodic irrotational surface waves in an inviscid fluid was first investigated by Stokes (1847). For irrotational waves the Stokes drift is positive everywhere, that is, it is in the same direction as the phase velocity (Longuet-Higgins and Stewart 1962; Eames and McIntyre 1999). The presence of vorticity in the wave field changes this, and may cause the Stokes drift to be negative (oppositely directed to the phase velocity) in some parts of the fluid. The vorticity related to the presence of viscosity is not important in this connection. Although the effect of viscosity induces a mean Eulerian drift velocity in the fluid, it only causes a slow attenuation of the Stokes drift through temporal or spatial amplitude decay (Weber 1983; Jenkins 1986). Thus, inclusion of viscosity does not cause any change of sign in the Stokes drift. Other sources of vorticity, for example, baroclinicity and the earth's rotation, have a much more profound influence. The effect of rotation on the Stokes drift has been investigated for two-dimensional horizontal flow by Longuet-Higgins (1969a) for double Kelvin waves, and by Weber and Drivdal (2012) for continental shelf waves (as part of a more comprehensive study), yielding positive Stokes drift where the bottom gradients are small, and negative drift over the steeper parts of the bottom topography. Negative Stokes drift has also been reported by Flierl (1981).

In this paper, we consider the effect of baroclinicity. The main purpose of the study is to investigate the apparent contradiction between the results from continuous stratification, which yields negative Stokes drift in parts of the fluid, and a two-layer model with constant

Corresponding author address: Jan Erik H. Weber, Department of Geosciences, University of Oslo, P.O. Box 1022 Blindern, 0315 Oslo, Norway.
E-mail: j.e.weber@geo.uio.no

DOI: 10.1175/JPO-D-13-0135.1

density in each layer. In the latter case, the Stokes drift is positive in both layers. The theory applies to internal plane waves in general, but we focus here on internal equatorial Kelvin waves because the equatorial regions display some of the strongest baroclinic signals in the ocean. The rest of this paper is organized as follows. In section 2, we present a short review of the Stokes drift for two-dimensional wave motion. In Section 3 we derive the Stokes drift in internal equatorial Kelvin waves, while in section 4 we specifically consider the equatorial Pacific. In Section 5, we investigate the (common) use of a two-layer structure for obtaining the baroclinic response. In Section 6 we discuss our results, and estimate a realistic value for the negative Stokes drift in the Pacific thermocline. Finally, section 7 contains some concluding remarks.

2. The Stokes drift in plane waves with vorticity

a. Particle motion in fluids

For didactic reasons, we give a short outline of the mathematical steps yielding the Stokes drift. A more comprehensive treatment is found in the pioneering study by Longuet-Higgins (1953). A Cartesian right-handed coordinate system (x, y, z) is chosen such that the z axis is vertical and directed upward. The corresponding unit vectors are $(\mathbf{i}, \mathbf{j}, \mathbf{k})$. The Stokes drift can be obtained by considering the Lagrangian velocity, which is the velocity of an individual fluid particle. We denote it by $\mathbf{v}_L$. Then, $\mathbf{v}_L(\mathbf{r}_0, t)$ is the velocity of a fluid particle whose position at time $t = t_0$ is $\mathbf{r}_0 = (x_0, y_0, z_0)$. At a later time t, the particle has moved to a new position

$$\mathbf{r}_L = \mathbf{r}_0 + D\mathbf{r} = \mathbf{r}_0 + \int_{t_0}^{t} \mathbf{v}_L(\mathbf{r}_0, t')\, dt'. \tag{1}$$

In an Eulerian description, where (x, y, z, t) are independent coordinates, the fluid velocity at time t is $\mathbf{v}(\mathbf{r}_L, t)$. Hence, consistency requires

$$\mathbf{v}_L(\mathbf{r}_0, t) = \mathbf{v}(\mathbf{r}_L, t). \tag{2}$$

By inserting for $\mathbf{r}_L$ from (1), and assuming that the distance $D\mathbf{r} = \mathbf{r}_L - \mathbf{r}_0$ traveled by the particle in the time interval $t - t_0$ is small, the two first terms of a Taylor expansion yields

$$\mathbf{v}_L(\mathbf{r}_0, t) = \mathbf{v}(\mathbf{r}_0, t) + \left[\int_{t_0}^{t} \mathbf{v}_L(\mathbf{r}_0, t')\, dt'\right] \cdot \nabla_L \mathbf{v}(\mathbf{r}_0, t), \tag{3}$$

where $\nabla_L \equiv \mathbf{i}\partial/\partial x_0 + \mathbf{j}\partial/\partial y_0 + \mathbf{k}\partial/\partial z_0$. The last part of the velocity on the right-hand side of (3) is often called the Stokes velocity $\mathbf{v}_S$, while the first term is the traditional Eulerian velocity at a fixed position. Hence, in general, $\mathbf{v}_L = \mathbf{v} + \mathbf{v}_S$. For waves with small wave steepness the difference between $\mathbf{v}_L$ and $\mathbf{v}$ is small, so to second order we can substitute the Lagrangian velocity by the Eulerian velocity in the integral in (3), that is,

$$\mathbf{v}_S = \left[\int_{t_0}^{t} \tilde{\mathbf{v}}(\mathbf{r}_0, t')\, dt'\right] \cdot \nabla_L \tilde{\mathbf{v}}(\mathbf{r}_0, t), \tag{4}$$

where the tilde denotes the linear periodic wave solution. In the same approximation, we can use $\mathbf{r}_0 = \mathbf{r}$ and $\nabla_L \equiv \mathbf{i}\partial/\partial x + \mathbf{j}\partial/\partial y + \mathbf{k}\partial/\partial z$. We thus see that the Stokes velocity to second order in wave steepness is determined completely by the linear Eulerian wave solution. For periodic waves, the drift (or net transport) is found by averaging over the wave cycle (denoted by an overbar). Then

$$\overline{\mathbf{v}}_L = \overline{\mathbf{v}} + \overline{\mathbf{v}}_S, \tag{5}$$

where $\overline{\mathbf{v}}_S$ is the Stokes drift, and $\overline{\mathbf{v}}$ is the mean Eulerian velocity.

The effect of friction is crucial in determining the mean Eulerian flow. For example, for temporally attenuated deep water surface gravity waves, the wave momentum is transferred to the mean Eulerian current through the action of a virtual wave stress at the surface (Longuet-Higgins 1969b; Weber and Førland 1990). For spatially damped waves, it is the wave-induced radiation stresses (see, e.g., Longuet-Higgins and Stewart 1962) that act to transfer wave momentum to the vertically averaged mean Lagrangian flow. A recent example here for long continental shelf waves is given in Weber and Drivdal (2012). This is very much in contrast to waves in an inviscid rotating ocean where the mean Lagrangian velocity may vanish identically—see Hasselmann (1970) for short surface waves and Moore (1970) for long waves in the shallow-water approximation. In these latter cases, the Stokes drift and the mean Eulerian current cancels exactly.

By using a Lagrangian formulation ab initio there are exact solutions in Lagrangian coordinates for inviscid plane waves where the individual fluid particles move in closed orbits, so the net Lagrangian current is zero—see Constantin (2001) and Weber (2012) for the Stokes edge wave and Constantin (2013) for short equatorial interfacial waves. These solutions are all variations of the classical Gerstner wave (Gerstner 1809). The Gerstner wave possesses vorticity in a homogenous inviscid ocean. For this reason such waves have received less attention in the literature.

In a turbulent ocean where the effect of friction is modeled by an eddy viscosity, the wave-induced mean Eulerian flow is difficult to assess, because it depends on the frictional decay of the wave field, as well as the effect of friction on the mean flow itself (particularly bottom friction in shallow water). The Stokes drift, on the other hand, is relatively easy to calculate as long as we can determine the linear wave field. Any effects of friction only appear through a slow change in wave amplitude. In the remainder of this paper, we focus on the Stokes drift. Further comments on the Stokes drift versus the mean Eulerian current are found in section 7 at the end of the paper.

b. The Stokes drift in plane waves

In this specific study of the Stokes drift we consider free (unforced) plane waves in a horizontally unlimited, incompressible inviscid ocean of constant depth H. The horizontal coordinate axes are situated at the undisturbed ocean surface, and the bottom is given by $z = -H$. The waves in our study are periodic, and propagate in the x direction with constant phase speed c without changing shape. There is no motion in the y direction, that is, $v = 0$. For such waves we must have that

$$\frac{\partial}{\partial x} = -\frac{1}{c}\frac{\partial}{\partial t}. \tag{6}$$

The horizontal Stokes drift $\overline{u}_S$ to second order in wave steepness becomes from (4):

$$\overline{u}_S = \overline{\left(\int \tilde{u}\, dt\right)\frac{\partial \tilde{u}}{\partial x}} + \overline{\left(\int \tilde{w}\, dt\right)\frac{\partial \tilde{u}}{\partial z}}, \tag{7}$$

because the lower limit in the integral is irrelevant here.

For irrotational two-dimensional wave motion, the velocity can be derived from a potential. In this case, $\partial u/\partial z = \partial w/\partial x$. Then, by applying (6):

$$\begin{aligned}\overline{u}_S &= -\frac{1}{c}\left\{\frac{\partial}{\partial t}\left[\overline{\left(\int \tilde{u}\, dt\right)\tilde{u}} + \overline{\left(\int \tilde{w}\, dt\right)\tilde{w}}\right] - \overline{\tilde{u}^2} - \overline{\tilde{w}^2}\right\} \\ &= \frac{1}{c}(\overline{\tilde{u}^2} + \overline{\tilde{w}^2}) > 0,\end{aligned} \tag{8}$$

which originally was derived by Longuet-Higgins and Stewart (1962). This result for the Stokes drift in irrotational waves was in fact proved by Eames and McIntyre (1999) to be exact, that is, not limited to second order in wave steepness. The forward drift in such waves has also been analyzed by Constantin (2006), and demonstrated experimentally by Umeyama (2012).

Along the lines of Eames and McIntyre (1999), it is easy to prove that the Stokes drift in the direction normal to the wave propagation direction is zero. For plane waves, the continuity equation reduces to

$$\frac{\partial u}{\partial x} + \frac{\partial w}{\partial z} = 0, \tag{9}$$

which allows us to introduce the streamfunction ψ, such that

$$u = -\frac{\partial \psi}{\partial z} \quad \text{and} \quad w = \frac{\partial \psi}{\partial x}. \tag{10}$$

Using (6), we have by definition

$$w = \frac{Dz}{dt} = \frac{\partial \psi}{\partial x} = -\frac{1}{c}\frac{\partial \psi}{\partial t} = \frac{1}{c}\left(-\frac{D\psi}{dt} + u\frac{\partial \psi}{\partial x} + w\frac{\partial \psi}{\partial z}\right), \tag{11}$$

where D/dt is the individual derivative following a fluid particle. From (10), the advective terms cancel. We integrate over the wave period T, and introduce the vertical particle displacement Z. Then, the vertical mean drift becomes:

$$\overline{w}_S = \frac{Z(T) - Z(0)}{T} = -\frac{1}{cT}[\psi(T) - \psi(0)] = 0, \tag{12}$$

because the Eulerian streamfunction ψ is periodic in time. This is an exact result, and is valid for waves with or without vorticity. Furthermore, the result does not depend on the boundary conditions for the streamfunction.

To obtain an expression for the horizontal Stokes drift that also includes cases with vorticity, we introduce the streamfunction into (7). Then

$$\overline{u}_S = \frac{1}{c}\left[\overline{\left(\frac{\partial \tilde{\psi}}{\partial z}\right)^2} + \overline{\tilde{\psi}\frac{\partial^2 \tilde{\psi}}{\partial z^2}}\right]. \tag{13}$$

For baroclinic motion in an ocean with constant depth H, we make the rigid-lid assumption, and take that

$$\tilde{\psi} = 0 \quad \text{and} \quad z = 0, -H. \tag{14}$$

This boundary condition is discussed in more detail in the next section where we specifically consider internal Kelvin waves in a stratified ocean. By integrating (13) in the vertical from the bottom to the surface, and utilizing the boundary conditions (14), we find for the Stokes flux that

$$\overline{U}_S = \int_{-H}^{0} \overline{u}_S \, dz = \frac{1}{c}\left[\overline{\int_{-H}^{0} \left(\frac{\partial\tilde{\psi}}{\partial z}\right)^2 dz} + \overline{\left(\tilde{\psi}\frac{\partial\tilde{\psi}}{\partial z}\right)_{-H}^{0}} - \overline{\int_{-H}^{0} \left(\frac{\partial\tilde{\psi}}{\partial z}\right)^2 dz}\right] = 0. \tag{15}$$

In the case of a rigid lid at the surface, a similar result is found in Longuet-Higgins (1969a) for the total mean volume flux in double Kelvin waves. From (13) we note that at the upper and lower boundaries, where $\tilde{\psi} = 0$, we have $\overline{u}_S > 0$. Accordingly, $\overline{u}_S$ must be negative in some parts of the interior in order to fulfill (15). To locate regions of negative Stokes drift, we must consider specific solutions for $\tilde{\psi}$.

The derivation of the Stokes drift (7) presupposes that the linear wave velocity is much larger than the Stokes drift velocity, that is, $|\overline{u}_S| \ll |\overline{\tilde{u}^2}|^{1/2} \sim \tilde{q}_0$. Using values at $z = 0$, where $\overline{u}_S$ is largest, we obtain from (13) that $|\overline{u}_S|/\tilde{q}_0 \sim \tilde{q}_0/c \ll 1$.

3. Internal equatorial Kelvin waves

There are few places in the world's oceans where the vertical stratification is greater than in the tropics (see, e.g., Levitus and Boyer 1994). The combination of a pronounced thermocline and the changing sign of the Coriolis parameter make the equatorial region a guide for various types of waves. These waves appear to be generated by temporal/spatial variations of the trade wind system. The eastward-propagating Kelvin wave is special in that the meridional wave velocity vanishes identically (see, e.g., Gill 1982) For nonzero meridional velocity, there exist an infinite number of equatorial waves with trapping scales on the same order as that for the Kelvin wave, that is, the Rossby radius of deformation (Matsuno 1966; Blandford 1966; Munk and Moore 1968).

Here, we consider the drift in free internal equatorial Kelvin waves, and direct the x axis along the equator toward the east, while the y axis points northward. For Kelvin waves, the corresponding velocity vector is $\mathbf{v} = (u, 0, w)$. We apply the beta-plane approximation for the Coriolis parameter, that is, $f = \beta y$, where $\beta = 2.3 \times 10^{-11}\,\mathrm{m^{-1}\,s^{-1}}$. Furthermore, we apply the Boussinesq approximation, assume incompressible flow, and take that the wavelength is much larger than the fluid depth, so we can make the hydrostatic assumption. Because we focus on the Stokes drift in this study, we neglect the effects of diffusive processes altogether.

The waves result from small perturbations from a state of rest characterized by a horizontally uniform stable stratification $\rho_0(z)$ in the gravity field. Details of this problem can be found in textbooks like LeBlond and Mysak (1978) or Gill (1982). Here, we give a very brief account. In principle, we expand our solutions in series after the wave steepness as a small parameter (but we retain our dimensional variables). The first-order (linear) equations for the conservation of momentum and density for an incompressible fluid are as follows:

$$\begin{aligned}
\frac{\partial\tilde{u}}{\partial t} &= -\frac{1}{\rho_r}\frac{\partial\tilde{p}}{\partial x},\\
\beta y\tilde{u} &= -\frac{1}{\rho_r}\frac{\partial\tilde{p}}{\partial y},\\
0 &= -\frac{1}{\rho_r}\frac{\partial\tilde{p}}{\partial z} - \frac{\tilde{\rho}}{\rho_r}g, \quad \text{and}\\
\frac{\partial\tilde{\rho}}{\partial t} &+ w\frac{d\rho_0}{dz} = 0,
\end{aligned} \tag{16}$$

where ρ_r is a constant reference density, and g is the acceleration due to gravity. Assuming separation of variables, we can write for the linear streamfunction $\tilde{\psi}$:

$$\tilde{\psi} = -cAF(y)\phi(z)\cos(kx - \omega t), \tag{17}$$

where A is the amplitude of the vertical displacement of the isopycnals, k is the wavenumber, and ω is the frequency. The corresponding phase speed is $c = \omega/k$. For equatorial Kelvin waves, one finds from (16)

$$F = \exp(-y^2/a^2). \tag{18}$$

Here,

$$a^2 = 2c/\beta, \tag{19}$$

where c must be positive (eastward wave propagation) for equatorial trapping to occur. The parameter $a = (2c/\beta)^{1/2}$ is referred to as the internal (or baroclinic) equatorial Rossby radius.

The z dependence in (17) can be written in terms of eigenfunctions in a numbered sequence ($n = 0, 1, 2, 3, \ldots$) —see, for example, Gill and Clarke (1974). Because the density difference across the sea surface is so much greater than the density differences within the ocean, one mode has quite a different character from the others. This is the barotropic mode ($n = 0$). It satisfies the condition of constant pressure along the sea surface, and the vertical velocity increases linearly from the bottom to the top. The speed of propagation is $c_0 = (gH)^{1/2}$. For the

remaining baroclinic modes ($n = 1, 2, 3, \ldots$), separation of variables leads to

$$\phi_n'' + \frac{N^2}{c_n^2}\phi_n = 0, \tag{20}$$

where primes denote differentiation with respect to z. In (20), N is the Brunt–Väisälä frequency defined by

$$N^2 = -\frac{g}{\rho_r}\frac{d\rho_0(z)}{dz}. \tag{21}$$

The eigenfunctions for the baroclinic modes are subject to vanishing vertical velocity at the top and bottom (see Gill and Clarke 1974):

$$\phi_n = 0 \quad \text{for} \quad z = 0, -H. \tag{22}$$

For a given $N(z)$, the solution yields separate constant eigenvalues c_1, c_2, c_3, etc., which represent the phase speed of the various baroclinic modes.

Inserting from (17) and (20) into (13), we obtain for the Stokes drift in internal equatorial Kelvin waves for mode n:

$$\overline{u}_{Sn} = \frac{c_n A_n^2}{2}\left(\phi'^2_n - \frac{N^2}{c^2}\phi_n^2\right)\exp(-2y^2/a_n^2). \tag{23}$$

Because ϕ_n is zero at the bottom and at the surface, and the Stokes flux must be zero, see (15), we realize from (23) that $\overline{u}_{Sn}$ must be negative in some parts of the interior fluid domain. More specifically, the z levels where $\overline{u}_{Sn}$ has extreme values ($\partial\overline{u}_{Sn}/\partial z = 0$) is given by

$$\phi_n(N'\phi_n + 2N\phi_n') = 0, \tag{24}$$

where we have utilized (20). Obviously, we have local maxima for $\phi_n(z) = 0$.

This kind of structure is most readily demonstrated if N is constant. We now obtain from (20) and (22):

$$\phi_n = \sin\left(\frac{Nz}{c_n}\right) \quad \text{and} \quad c_n = \frac{HN}{n\pi}, \quad \text{for} \quad n = 1, 2, 3, \ldots \tag{25}$$

By inserting into (23):

$$\overline{u}_S = \frac{\pi N}{2H}\sum_{n=1}^{\infty} nA_n^2 \cos\left(\frac{2n\pi}{H}z\right)\exp(-2y^2/a_n^2). \tag{26}$$

We notice that the drift due to the first mode ($n = 1$) has its largest negative value in the middle of the layer. In Fig. 1 we have plotted the nondimensional Stokes drift for the first two modes, scaling by the factor $u_0 = \pi N n A_n^2/(2H)$.

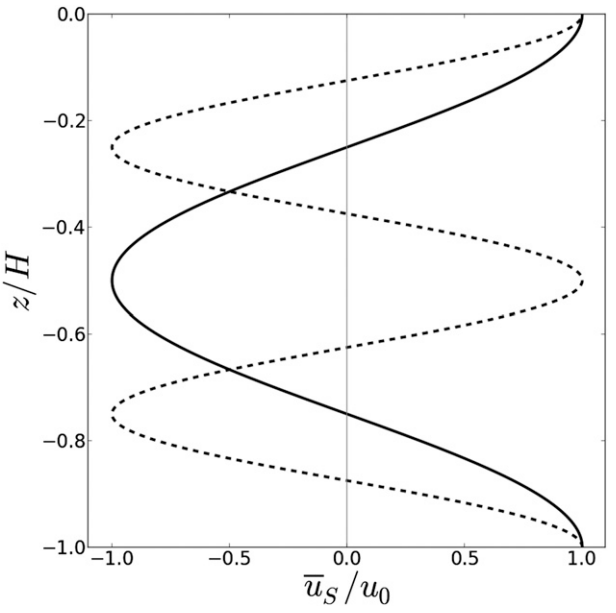

FIG. 1. The first (solid line) and second mode (broken line) for the nondimensional Stokes drift for constant N at $y = 0$.

For a more realistic distribution of the density field, the eigenvalue problem must be solved numerically. We return to this problem in the next section.

We close this section with a comment on the Stokes drift for the barotropic mode. For shallow-water surface waves with amplitude A_0 and phase speed $c_0 = (gH)^{1/2}$, it can be written (see, e.g., Phillips 1977):

$$\overline{u}_{S_0} = \frac{c_0 A_0^2}{2H^2}. \tag{27}$$

Inserting for the first mode $n = 1$ in (26) at the surface along the equator, we find the ratio

$$\left|\frac{\overline{u}_{S_0}}{\overline{u}_{S_1}}\right| = \frac{c_0 A_0^2}{\pi^2 c_1 A_1^2}. \tag{28}$$

Typical orders of magnitude here are $c_0 \sim 100\,\mathrm{m\,s^{-1}}$, $A_0 \sim 1\,\mathrm{m}$, and $c_1 \sim 2\,\mathrm{m\,s^{-1}}$, $A_1 \sim 50\,\mathrm{m}$. We realize immediately that the ratio (28) is much less than unity, justifying the neglect of the barotropic mode in this connection.

4. Application to the equatorial Pacific

As far as equatorial dynamics are concerned, it is the Pacific Ocean that has attracted most interest among researchers, and where most data have been collected.

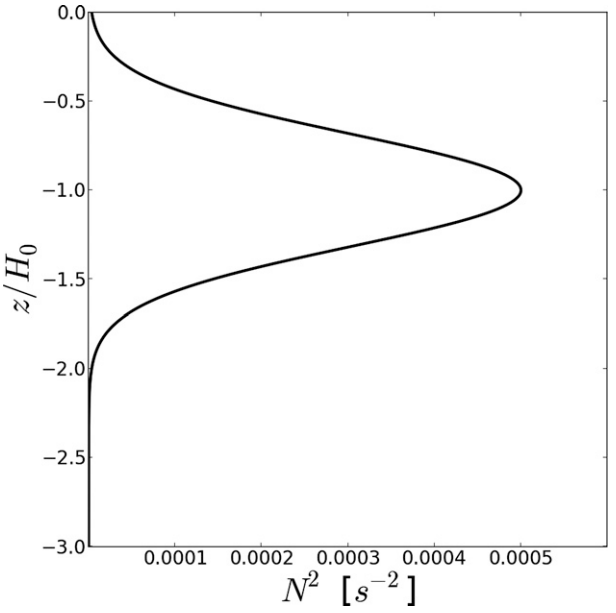

FIG. 2. Idealized distribution of $N^2(z)$ for the equatorial Pacific from (29) with $b = 5$.

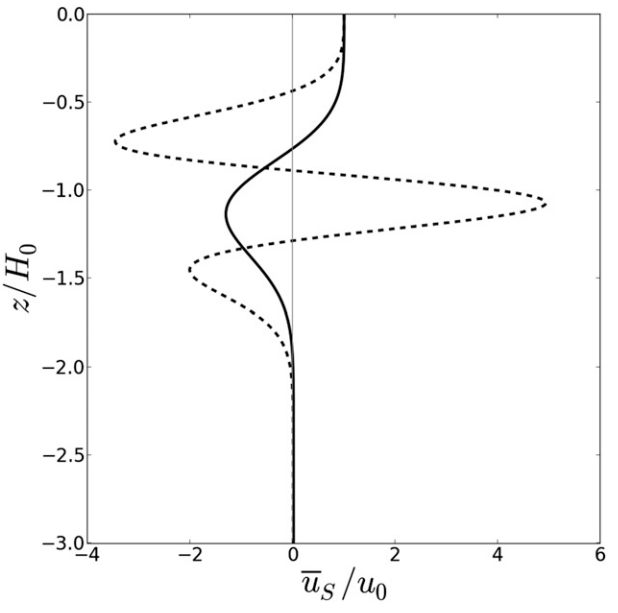

FIG. 3. The nondimensional Stokes drift at the equator vs z/H_0 for the first (solid line) and second mode (broken line) when N is given by (29).

Evidently, the Brunt–Väisälä frequency is far from constant in the Pacific equatorial thermocline (see, e.g., Colin et al. 1971). We simplify, and approximate the shape of $N^2(z)$ by a Gaussian function:

$$N^2(z) = N_0^2 \exp[-b(z/H_0 + 1)^2]. \tag{29}$$

From Philander (1981), we take that $N_0^2 = 5 \times 10^{-4}\,\mathrm{s}^{-2}$. The depth H_0, where $N^2(z)$ attains a maximum, is approximately 150 m (Kessler 2005). Furthermore, b is a dimensionless coefficient. In Fig. 2, we have depicted (29) for $b = 5$.

With $N^2(z)$ given by (29), (20) and (22) are easily solved by a simple shooting method. For the first mode we find $c_1 = 2.6\,\mathrm{m\,s}^{-1}$, which fits well with previously reported values (Wunsch and Gill 1976; Kessler and McPhaden 1995). Calculations for the next two modes yield $c_2 = 0.77\,\mathrm{m\,s}^{-1}$, and $c_3 = 0.46\,\mathrm{m\,s}^{-1}$, respectively. These latter values are somewhat smaller than those reported by Kessler and McPhaden (1995) from the Hawaii–Tahiti Shuttle Experiment ($c_1 = 2.73$, $c_2 = 1.74$, and $c_3 = 1.06\,\mathrm{m\,s}^{-1}$, respectively). However, we do not intend to model the equatorial thermocline precisely at any specific longitude. Our main aim is to investigate theoretically the principle differences between the Stokes drift for the first baroclinic mode for a constant N, a peaked N, and a discontinuous density distribution. Hence, we are content by using an idealized Brunt–Väisälä frequency distribution, which yields satisfactory results for the lowest mode.

At the equator ($y = 0$), the numerical values of the eigenfunctions $\phi_1(z)$ and $\phi_2(z)$ are inserted into (23). The resulting nondimensional Stokes drift for these two modes is plotted in Fig. 3. In this case, the scaling factor is $u_0 = c_n A_n^2/(2H_0^2)$.

For constant N, the Stokes drift is symmetric about the midlayer depth, as seen in Fig. 1, where the first mode has its largest negative value. For a peaked N, the negative Stokes drift for the first mode typically occurs in the region where $N^2(z)$ has its maximum. Obviously, the region of negative drift will be more narrow when $N^2(z)$ becomes more peaked. This will be discussed further in section 6. The Stokes drift for the second mode when we have $N^2(z)$ shows the same qualitative behavior as for constant N, but the maximum positive value in the interior now occurs in the region where $N^2(z)$ has its maximum, with negative values above and below this level.

5. The two-layer model

Kessler and McPhaden (1995) report that both the first and second mode of the Kelvin wave are important for explaining the displacement of the equatorial thermocline, while the third and fourth modes could be discarded. Here we concentrate on the first baroclinic mode, because this is directly relevant for the comparison with results from a two-layer model in which all baroclinic modes, except the first (interfacial mode), are suppressed.

In discussing the dynamics of the equatorial region, a reduced-gravity model is often applied (McCreary 1976; Busalacchi and O'Brien 1980; Boyd 1980). In this approach there are two layers of constant density, where the upper is thin and active, and the lower is deep and with negligible velocity (i.e., a so-called 1.5-layer model). Then, by replacing the acceleration due to gravity by the reduced gravity, the various trapped baroclinic equatorial waves follow directly from the discussion in Gill's book (Gill 1982).

We consider a two-layer model with constant densities ρ_1 and ρ_2 in the upper and lower layer, respectively. The interface is placed at depth H_0, where we, in the continuous case, have a peak in N^2. For long Kelvin waves, using the hydrostatic approximation, one finds for the baroclinic response in the upper layer (see, e.g., Gill 1982):

$$\frac{\partial \tilde{U}_1}{\partial t} = c_1^2 \frac{\partial \tilde{\xi}_1}{\partial x},$$

$$\beta y \tilde{U}_1 = c_1^2 \frac{\partial \tilde{\xi}_1}{\partial y}, \quad \text{and}$$

$$\frac{\partial \tilde{\xi}_1}{\partial t} = \frac{\partial \tilde{U}_1}{\partial x}. \tag{30}$$

Here, $\tilde{\xi}_1$ is the displacement of the interface from its original position $z = -H_0$, and $\tilde{U}_1$ is the volume flux. Furthermore, we have defined

$$c_1 = \left[\frac{g\Delta\rho}{\rho} \frac{(H - H_0)H_0}{H} \right]^{1/2}. \tag{31}$$

We have here taken that $\Delta\rho = \rho_2 - \rho_2$ and $\rho = \rho_1 \approx \rho_2$. For baroclinic motion, the volume flux $\tilde{U}_2$ in the lower layer is given by $\tilde{U}_2 = -\tilde{U}_1$.

The solution to this problem is readily obtained. For periodic waves with phase speed $c_1 = \omega/k$, we find for the interfacial Kelvin wave

$$\tilde{\xi}_1 = A \exp(-y^2/a_1^2) \cos(kx - \omega t), \tag{32}$$

where a_1 is the interfacial equatorial Rossby radius given by $a_1 = (2c_1/\beta)^{1/2}$. The velocities in the upper and lower layer become

$$\tilde{u}_1 = \frac{\tilde{U}_1}{H_0} = -\frac{c_1 A}{H_0} \exp(-y^2/a_1^2) \cos(kx - \omega t) \quad \text{and}$$

$$\tilde{u}_2 = \frac{\tilde{U}_2}{H - H_0} = \frac{c_1 A}{H - H_0} \exp(-y^2/a_1^2) \cos(kx - \omega t). \tag{33}$$

For the two-layer approach in the nonrotating case one can use potential theory in both layers (Phillips 1977),

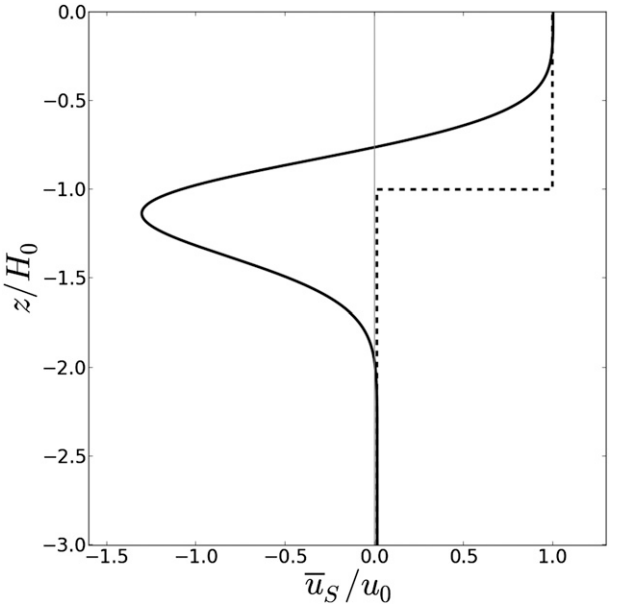

FIG. 4. The nondimensional Stokes drift vs z/H_0 for the first mode when N is given by (29) (solid line), and for the interfacial wave in a two-layer model (dashed line).

and hence, according to (8), the Stokes drift becomes positive everywhere. The same applies to equatorial Kelvin waves. In each layer of constant density, we find $\partial\tilde{u}/\partial z - \partial\tilde{w}/\partial x = 0$, so the x and z dependence can be derived from a potential. By inserting from (33) for long waves into (7), we obtain for the Stokes drift:

$$\overline{u}_{S_1} = \frac{c_1 A^2}{2H_0^2} \exp(-y^2/a_1^2) \quad \text{for} \quad 0 \geq z > -H_0 \quad \text{and}$$

$$\overline{u}_{S_2} = \frac{c_1 A^2}{2(H - H_0)^2} \exp(-y^2/a_1^2) \quad \text{for} \quad -H_0 > z \geq -H. \tag{34}$$

Scaling the two-layer result such that the drift equals one in the upper layer at $y = 0$, it becomes $H_0^2/(H - H_0)^2$ in the lower layer. The result (34) is plotted in Fig. 4, together with $\overline{u}_S$ for the more realistic equatorial stratification (29).

We note from Fig. 4 that the Stokes drift in the two cases is very different. In particular, the two-layer model fails to produce a region of negative Stokes drift. This is a matter of concern, because reduced gravity models in the ocean, with negligible motion in the lower deep layer, often are used to represent the first baroclinic internal mode. This obviously introduces a serious error as far as the nonlinear wave drift is concerned.

6. Discussion

If we introduce the vertical displacement $\tilde{\xi}$ of the isopycnals, we have from linearized theory that $\partial\tilde{\xi}/\partial t = \tilde{w} = \partial\tilde{\psi}/\partial x$. By utilizing (6), we obtain $\tilde{\xi} = -\tilde{\psi}/c$. Inserting into (13), we find for the Stokes drift

$$\overline{u}_S = \frac{1}{c}\overline{\tilde{u}^2} + \overline{\tilde{\xi}\frac{\partial\tilde{u}}{\partial z}}. \tag{35}$$

In general, we have that $\partial\tilde{u}/\partial z < 0$ when $\tilde{\xi} > 0$, so the last term is negative [in a two-layer model we have $\tilde{u}_2 > 0$ below an interfacial crest $\tilde{\xi}_1 > 0$, and $\tilde{u}_1 < 0$ above it—see (32) and (33)]. Because the vorticity component $\tilde{\zeta}$ in the y direction is given by $\tilde{\zeta} = \partial\tilde{u}/\partial z - \partial\tilde{w}/\partial x$, and $\partial\tilde{w}/\partial x$ is very small for long waves, it is actually the vorticity that appears in the last term of (35). In this case the vertical displacement is continuous, and the horizontal velocity components are finite at both sides of the interface. A two-layer structure for the density then implies an infinite vorticity at the interface. From (35) we note that the Stokes drift then would become negative, and infinitely large, in an infinitely thin layer. However, the negative Stokes flux must be finite, and cancel the sum of the positive Stokes fluxes in the upper and lower layer, as required by (15). Hence, the negative Stokes drift necessarily must exhibit a delta-function behavior at the interface in the two-layer limit.

Obviously, an infinitely large negative Stokes drift is an unphysical result, and will not be observed in nature. In laboratory experiments with a two-layer structure, the molecular viscosity cannot be neglected, and will probably prevent large horizontal drift velocities near the interface. In the ocean, a too-steep pycnocline may promote instability. Denoting the magnitude of the shear of the linear wave field by dU/dz at the depth H_0, where $N_{\max} = N_0$, we obtain from Phillips (1977) in the long-wave approximation

$$\frac{dU}{dz} = \frac{N_0^2}{\omega}kA. \tag{36}$$

Hence, the local gradient Richardson number becomes

$$\mathrm{Ri} = \frac{N_0^2}{(dU/dz)^2} = \left(\frac{c}{N_0 A}\right)^2. \tag{37}$$

We note that for a sufficiently large amplitude of the interfacial disturbance, a narrow-peaked N may lead to such small values of Ri that shear instability could result. Classic theory states that instability of inviscid stratified shear flow may occur when $\mathrm{Ri} < 1/4$ (Miles 1961; Howard 1961), while for symmetric instability of nondiffusive stratified geostrophic flow one must require $\mathrm{Ri} < 1$ (Stone 1966). From Colin et al. (1971), a maximum displacement A of the isotherms of more than 50 m from a mean horizontal position does not seem unrealistic. In fact, Kessler and McPhaden (1995) report that the observed depth of the 20°C thermocline varied between 80 and 180 m. For the example in section 4 with $c = 2.6\,\mathrm{m\,s^{-1}}$ and $N_0^2 = 5\times10^{-4}\,\mathrm{s^{-2}}$, a middle-of-the-road value $A = 65$ m leads to $\mathrm{Ri} = 1.8$. Hence, it is not likely that the shear in these long waves may lead to instability and subsequent turbulent mixing.

In dimensional terms, the values of the depicted Stokes drift (first mode) for variable N in Figs. 3 and 4 must be multiplied by the factor $u_0 = c_1 A_1^2/(2H_0^2)$. Then, with our previously applied values $H_0 = 150$ m, $A_1 = 65$ m, and $c_1 = 2.6\,\mathrm{m\,s^{-1}}$, we find for the scaling factor: $u_0 = 0.24\,\mathrm{m\,s^{-1}}$. Hence, from Fig. 4 we obtain that

$$\overline{u}_S(y = 0, z = -H_0) = -1.34u_0 \approx -0.32\,\mathrm{m\,s^{-1}}. \tag{38}$$

This order of magnitude is comparable to observed values of the Equatorial Undercurrent at the level of the thermocline (Taft et al. 1974).

The basic problem with layered models is that the flow is irrotational in each layer, yielding a positive Stokes drift everywhere. It would not help to add infinitely many homogeneous layers. However, if we added an intermediate layer with a linear density decrease, we would find a backward Stokes drift in this layer. But in this case the density distribution would just be a piecewise approximation to the continuous profile leading to (29).

7. Concluding remarks

In recent years, a considerable number of papers have been devoted to a direct computation of the Lagrangian or quasi-Lagrangian mean velocity in waves (e.g., Andrews and McIntyre 1978; Weber 1983; Jenkins 1986; Weber et al. 2006; Broström et al. 2008). In such analyses the Stokes drift turns out to be an inherent part of the full Lagrangian wave-induced mean drift. The remaining part can be interpreted as a quasi-Eulerian mean flow, confirming Longuet-Higgins' earlier result (Longuet-Higgins 1953). However, the mean Eulerian current depends on turbulent eddy viscosity, which in turn depends on the sea state, and the results are ridden by the uncertainty of assessing the eddy viscosity magnitude and spatial distribution. This is not so for the Stokes drift, which is inherent in the waves, and can be determined in reliable way. Also, in many cases, the Stokes drift is of the same order of magnitude as the mean Eulerian current, which makes it an important contributor to the

mean oceanic circulation. In addition, one extremely simplifying aspect is that the Stokes drift to a good approximation can be obtained from the inviscid fluid motion.

From the present study of internal equatorial Kelvin waves, the drift results for the Pacific Ocean are particularly interesting. Here, the Equatorial Undercurrent extends down into the upper part of the thermocline (Cromwell et al. 1954). Observed values of the undercurrent in the thermocline (Taft et al. 1974) are of the same order of magnitude as the negative Stokes drift derived in this paper. Obviously, Lagrangian measurements that can resolve the Stokes drift contribution to the mass transport velocity in the equatorial thermocline are needed.

Acknowledgments. We gratefully acknowledge financial support from the Research Council of Norway through the Grants 196438 (BioWave) and 207541 (OilWave).

REFERENCES

Andrews, D. G., and M. E. McIntyre, 1978: An exact theory of nonlinear waves on a Lagrangian-mean flow. *J. Fluid Mech.,* **89,** 609–646.

Blandford, R., 1966: Mixed gravity–Rossby waves in the ocean. *Deep-Sea Res.,* **13,** 941–961.

Boyd, J. P., 1980: The nonlinear equatorial Kelvin wave. *J. Phys. Oceanogr.,* **10,** 1–11.

Broström, G., K. H. Christensen, and J. E. H. Weber, 2008: A quasi-Eulerian, quasi- Lagrangian view of surface wave–induced flow in the ocean. *J. Phys. Oceanogr.,* **38,** 1122–1130.

Busalacchi, A. J., and J. J. O'Brien, 1980: The seasonal variability in a model of the tropical Pacific. *J. Phys. Oceanogr.,* **10,** 1929–1951.

Colin, C., C. Henin, P. Hisard, and C. Oudot, 1971: Le courant de Cromwell dans le Pacifique central en Février 1970. *Cah. ORSTOM Ser. Océanogr.,* **9,** 167–186.

Constantin, A., 2001: Edge waves along a sloping beach. *J. Phys.,* **34A,** 9723–9731.

——, 2006: The trajectories of particles in Stokes waves. *Invent. Math.,* **166,** 523–535.

——, 2013: Some three-dimensional nonlinear equatorial flows. *J. Phys. Oceanogr.,* **43,** 165–175.

Cromwell, T., R. B. Montgomery, and E. D. Stroup, 1954: Equatorial Undercurrent in Pacific Ocean revealed by new methods. *Science,* **119,** 648–649.

Eames, I., and M. E. McIntyre, 1999: On the connection between Stokes drift and Darwin drift. *Math. Proc. Cambridge Philos. Soc.,* **126,** 171–174.

Flierl, G. R., 1981: Particle motions in large-amplitude wave fields. *Geophys. Astrophys. Fluid Dyn.,* **18,** 39–74.

Gerstner, F., 1809: Theorie der Wellen samt einer daraus abgeleiteten Theorie der Deichprofile. *Ann. Phys.,* **2,** 412–455.

Gill, A. E., 1982: *Atmosphere–Ocean Dynamics*. Academic Press, 662 pp.

——, and A. J. Clarke, 1974: Wind-induced upwelling, coastal currents and sea-level changes. *Deep-Sea Res.,* **21,** 325–345.

Hasselmann, K., 1970: Wave-driven inertial oscillations. *Geophys. Fluid Dyn.,* **1,** 463–501.

Howard, L. N., 1961: Note on a paper of John W. Miles. *J. Fluid Mech.,* **10,** 509.

Jenkins, A. D., 1986: A theory for steady and variable wind- and wave-induced currents. *J. Phys. Oceanogr.,* **16,** 1370–1377.

Kessler, W. S., 2005: The oceans. *Intraseasonal Variability in the Atmosphere-Ocean Climate System,* W. K. M. Lau and D. E. Waliser, Eds., Springer Praxis Books, 175–222.

——, and M. J. McPhaden, 1995: Oceanic equatorial waves and the 1991/93 El Niño. *J. Climate,* **8,** 1757–1774.

LeBlond, P. H., and L. A. Mysak, 1978: *Waves in the Ocean.* Elsevier, 602 pp.

Levitus, S., and T. Boyer, 1994: *Temperature.* Vol. 4, *World Ocean Atlas 1994,* NOAA Atlas NESDIS 4, 117 pp.

Longuet-Higgins, M. S., 1953: Mass transport in water waves. *Phil. Trans. Roy. Soc. London,* **A245,** 535–581.

——, 1969a: On the transport of mass by time-varying ocean currents. *Deep-Sea Res.,* **16,** 431–447.

——, 1969b: A nonlinear mechanism for the generation of sea waves. *Proc. Roy. Soc. London,* **A311,** 371–389.

——, and R. W. Stewart, 1962: Radiation stress and mass transport in gravity waves, with application to ''surf beats.'' *J. Fluid Mech.,* **13,** 481–504.

Matsuno, T., 1966: Quasi-geostrophic motions in the equatorial area. *J. Meteor. Soc. Japan Ser. II,* **44,** 25–43.

McCreary, J., 1976: Eastern tropical ocean response to changing wind systems: With application to El Niño. *J. Phys. Oceanogr.,* **6,** 632–645.

Miles, J. W., 1961: On the stability of heterogeneous shear flows. *J. Fluid Mech.,* **10,** 496.

Moore, D., 1970: The mass transport velocity induced by free oscillations at a single frequency. *Geophys. Fluid Dyn.,* **1,** 237–247.

Munk, W., and D. Moore, 1968: Is the Cromwell current driven by equatorial Rossby waves? *J. Fluid Mech.,* **33,** 241–259.

Philander, S. G. H., 1981: The response of equatorial oceans to a relaxation of the trade winds. *J. Phys. Oceanogr.,* **11,** 176–189.

Phillips, O. M., 1977: *The Dynamics of the Upper Ocean.* 2nd ed. Cambridge University Press, 269 pp.

Stokes, G. G., 1847: On the theory of oscillatory waves. *Trans. Cambridge Philos. Soc.,* **8,** 441–455.

Stone, P. H., 1966: On nongeostrophic baroclinic stability. *J. Atmos. Sci.,* **23,** 390–400.

Taft, B. A., B. M. Hickey, C. Wunsch, and D. J. Baker, 1974: Equatorial undercurrent and deeper flows in the central Pacific. *Deep-Sea Res.,* **21,** 403–430.

Umeyama, M., 2012: Eulerian–Lagrangian analysis for particle velocities and trajectories in a pure wave motion using particle image velocimetry. *Philos. Trans. Roy. Soc.,* **A370,** 1687–1702.

Weber, J. E., 1983: Attenuated wave-induced drift in a viscous rotating ocean. *J. Fluid Mech.,* **137,** 115–129.

——, 2012: A note on trapped Gerstner waves. *J. Geophys. Res.,* **117,** C03048, doi:10.1029/2011JC007776.

——, and E. Førland, 1990: Effect of air on the drift velocity of water waves. *J. Fluid Mech.,* **218,** 619–640.

——, and M. Drivdal, 2012: Radiation stress and mean drift in continental shelf waves. *Cont. Shelf Res.,* **35,** 108–116.

——, G. Broström, and Ø. Saetra, 2006: Eulerian versus Lagrangian approaches to wave-induced transport in the upper ocean. *J. Phys. Oceanogr.,* **36,** 2106–2118.

Wunsch, C., and A. E. Gill, 1976: Observations of equatorially trapped waves in the Pacific sea level variations. *Deep-Sea Res.,* **23,** 371–390.